



Termination Shock Particle Streaming Upstream at New Horizons

Erick Powell¹, Merav Opher¹, Ethan Bair¹, Matthew Hill², Romina Nikoukar², Joe Giacalone³, Konstantinos Dialynas⁴, John D. Richardson⁵, Pontus C. Brandt², Kelsi N. Singer⁶, S. Alan Stern⁶, Elena Provornikova², Anne J. Verbiscer^{6,7}, Andrew R. Poppe⁸, Joel Wm. Parker⁶ and New Horizons Heliospheric Team

¹Astronomy Department, Boston University, Boston, MA, USA; empowell@bu.edu

²Johns Hopkins Applied Physics Laboratory, Laurel, MD, USA

³Lunar & Planetary Laboratory, University of Arizona, Tucson, AZ 85721, USA

⁴Center for Space Research and Technology, Academy of Athens, Athens, Greece

⁵Kavli Institute for Astrophysics and Space Research and Department of Physics, Massachusetts Institute of Technology, Cambridge, MA, USA

⁶Southwest Research Institute, Boulder, CO, USA

⁷Department of Astronomy, University of Virginia, Charlottesville, VA, USA

⁸Space Sciences Laboratory, University of California, Berkeley, CA, USA

Received 2024 December 02; accepted 2024 December 10; published 2024 December 27

Abstract

A couple years before Voyager 1 and Voyager 2 (V2) crossed the termination shock (TS), instruments on board both spacecraft observed high intensities of accelerated termination shock particles (TSPs) beaming in opposite directions. This phenomenon was explained by magnetic field lines connecting the spacecraft to the TS prior to the crossings. The opposite streaming of TSPs is due to an east–west asymmetry of the TS caused by the interstellar magnetic field building up on the outside of the heliopause. Here, we examine the magnetic connectivity for New Horizons (NH) ahead of the TS with a global MHD model with steady solar wind conditions. Our model predicts that NH will observe particles streaming in the same direction as V2 (+ T direction in the RTN coordinate system), 1.0 ± 0.7 au from the TS. We then estimate the average speed of the TS during the V2 TS crossing to be 2.5 au yr^{-1} outward, based on the timing and distance of the TS at the onset of the TSP observations and the crossing itself. Using this speed, we find that NH will have a 0.2 yr warning prior to crossing the TS if the TS is moving inward at the time of the crossing and a 2.4 yr warning if the TS is moving outward.

Unified Astronomy Thesaurus concepts: Termination shock (1690); Heliosphere (711); Heliosheath (710); Solar wind (1534); Solar cycle (1487)

1. Introduction

The nature of the heliosphere is governed by both solar wind and local interstellar medium (ISM) conditions. The fully ionized solar wind accelerates radially from the surface of the Sun to supersonic speeds. The Sun moves at a speed of about $\sim 26 \text{ km s}^{-1}$ relative to the local ISM (M. Witte 2004; E. Möbius et al. 2009). The theoretical foundations of heliophysics were pioneered using idealized assumptions about the solar wind and interstellar conditions (L. Davis 1955; E. N. Parker 1961; W. I. Axford 1972). Early analyses suggested that the heliosphere resembled a comet with a long tail (V. B. Baranov & Y. G. Malama 1993). However, recent theory, modeling, and measurements from the Voyagers and Cassini have challenged this paradigm (J. F. Drake et al. 2015; M. Opher et al. 2015; K. Dialynas et al. 2017). M. Opher et al. (2015) argue that an ideal Parker spiral magnetic field can play an active role in confining the plasma in the heliosheath, rather than the passive role previously assumed. This results in a “croissant-like” two-lobe heliosphere. V. V. Izmodenov & D. B. Alexashov (2015) and N. V. Pogorelov et al. (2015) present other models that also see this confinement, but both argue for a long-tailed heliosphere, unlike the croissant model.

Interstellar neutrals, primarily hydrogen and helium, travel to and then through the heliosphere unaffected by heliospheric and interstellar magnetic fields. These interstellar neutrals are

mostly unaffected by collisions within the heliosphere, since the mean free path for charge exchange for interstellar hydrogen is hundreds of astronomical units ($1 \text{ au} = 150 \times 10^6 \text{ km}$; V. V. Izmodenov et al. 2000). This allows neutral hydrogen atoms to travel mostly unimpeded through the heliosphere before undergoing charge exchange with plasma from the solar wind or ISM. Although individual neutral hydrogen atoms have a low probability of undergoing charge exchange, they play an important role in shaping the structure of the heliosphere (K. Dialynas et al. 2022; A. Galli et al. 2022) due to the relatively high density of neutral hydrogen atoms, $\sim 0.127 \text{ cm}^{-3}$ at the termination shock (TS; P. Swaczyna et al. 2020), streaming through the heliosphere.

Along with interstellar neutrals, magnetic fields in the ISM and solar wind play critical roles in shaping the heliosphere. As discussed by M. Opher et al. (2015), the solar magnetic field collimates the plasma in the heliosheath. The interstellar magnetic field is significant because the interstellar flow velocity is near the superfast magnetosonic velocity of the ISM, and as a result, minor changes in the interstellar magnetic field can create major differences in the ISM, such as if there is a bow shock or bow wave in front of the heliosphere (B. Zieger et al. 2013) and the width and density profile of the hydrogen wall (G. P. Zank et al. 2013).

In situ observations of the heliospheric boundaries are rare but essential for understanding the processes that occur within the heliosphere. Voyager 1 (V1) and Voyager 2 (V2) are the only spacecraft to have left the heliosphere while operational; they made the first in situ observations of the TS and heliopause (HP; S. M. Krimigis et al. 2019). V1 first crossed

the TS in 2004 December at 94.0 au (L. F. Burlaga et al. 2005; R. B. Decker et al. 2005; E. C. Stone et al. 2005), and in 2007 August, V2 first crossed the TS at 83.7 au (L. F. Burlaga et al. 2008; R. B. Decker et al. 2008; E. C. Stone et al. 2008). Reproducing these observations is crucial for validating models of the heliosphere. The TS was crossed 10 au closer to the Sun in the southern hemisphere than in the northern hemisphere.

In mid-2002, as V1 approached the TS, strong particle beaming was observed in both the Low Energy Charged Particle (LECP) instrument (R. B. Decker et al. 2005) and Cosmic Ray Subsystem (CRS; E. C. Stone et al. 2005) in the $-T$ direction in the radial–tangential–normal coordinate system (RTN; where R direction is in the radial direction from the Sun to the spacecraft, T is defined by the cross product of the solar rotation axis and R , and N is the normal right-hand complement). The observed particle intensity decreased significantly in 2003 and then reappeared at the beginning of 2004, steadily intensifying until the TS crossing.

In contrast, in 2005, as V2 approached the TS, LECP (R. B. Decker et al. 2008) and CRS (E. C. Stone et al. 2008) observed strong beaming in the $+T$ direction. This particle beaming was consistently observed from 2005 until the TS crossing in 2007. For both spacecraft, particle beaming was observed in ions with energies ranging from 28 keV to several MeV.

Figure 1 shows the LECP observations as V1 and V2 approached the TS for a single energy channel (53–85 keV for V1 and 40–80 keV for V2). Panel (A) shows the observations of the LECP sectors facing the $+T$ and $-T$ directions for V1 as the spacecraft approached the TS. Panel (B) shows the ratio of these two sectors, highlighting strong beaming in the $-T$ direction. Panels (C) and (D) show the same for V2 as it approached the TS, showing beaming in the $+T$ direction, opposite to what was observed by V1.

J. R. Jokipii & J. Giacalone (2004) suggested that this beaming can be explained by the bluntness of the TS. Spacecraft can be connected to the TS via magnetic field lines, allowing them to observe streaming termination shock particles (TSPs) flowing along these field lines from the TS. Subsequent studies showed that bluntness alone is not sufficient to explain the observations, but an additional east–west asymmetry is needed. This asymmetry is caused by the interstellar magnetic field pressure at the HP (M. Opher et al. 2006, 2007, 2009b).

The first quantitative investigation of this effect, along with the east–west asymmetries of the TS, was conducted by M. Opher et al. (2006). This study was able to explain the observed direction of beaming for V1, predict the direction of beaming for V2, and accounted for the closer distance to the TS in the southern hemisphere (R. B. Decker et al. 2008; E. C. Stone et al. 2008). Further investigations using similar methods were able to constrain the strength and direction of the interstellar magnetic field (M. Opher et al. 2007). M. Opher et al. (2009b) revisited the previous work using a four-fluid treatment of neutral hydrogen and saw qualitatively similar asymmetries but did not quantify the differences. These constraints were done with uniform solar wind conditions.

However, the TS is fundamentally time dependent as the solar wind varies in time (H. Washimi et al. 2007; J. D. Richardson & C. Wang 2011; E. Provornikova et al. 2014; V. V. Izmodenov & D. B. Alexashov 2020). In the case of V1 and V2, the difference in the observed distances to the TS at V1 and V2 of 10 au was argued to be only 7–8 au when accounting for the

motion of the TS (J. D. Richardson et al. 2008), the rest due to the interstellar magnetic field pressure (M. Opher et al. 2006, 2007; N. V. Pogorelov et al. 2007).

New Horizons (NH) is now fast approaching the TS and is expected to measure pickup ions (with energies of \sim keV, where Voyager could measure ions of up to a few keV and >30 keV; however, the fluxes of pickup ions in the outer heliosphere were too small to be observed) for the first time at the TS. The instruments on board will provide an unparalleled view of the TS and the processes that occur at and near it. Understanding what observations will be made, how much warning there will be of the crossing, and how soon to expect these observations is essential to maximize science output. This presents an opportunity to estimate how far in advance NH will observe TSPs with the techniques that were able to reproduce the streaming before the V1 crossing and predict that ahead of the V2 crossing.

The Letter is organized as follows. Section 2 presents the heliosphere model used for this investigation, including a brief description of the differences compared to the MHD model used by M. Opher et al. (2006, 2007, 2009b), as well as a description of the technique used for the analysis. Section 3 presents the results of the model analysis, comparing the observations from V1 and V2 with the model results and providing predictions for the upcoming NH TS crossing. Section 4 explores the implications of these results for the TS crossing and discusses the limitations of the modeling. Finally, Section 5 presents a summary of the results.

2. Modeling

The numerical model used for this work is the outer heliosphere component of the Space Weather Modeling Framework (G. Tóth et al. 2005). This model is a 3D multifluid MHD code adapted from the Block-Adaptive Tree Solar wind Roe–Type Scheme code (M. Opher et al. 2003, 2006; 2009a, 2020; G. Tóth et al. 2012). It evolves multiple plasma and neutral hydrogen fluids with charge-exchange source terms that self-consistently couple the fluids. Two previous iterations of this model have been used to investigate TSP streaming. The model used in M. Opher et al. (2006, 2007) was a pure MHD model that did not consider neutral hydrogen. In contrast, M. Opher et al. (2009b) revisited this effect with a model that considered neutral hydrogen, using a four-fluid treatment, with a fluid for each of the distinct regions of the heliosphere. The implementation of the four-fluid neutral hydrogen model is first described and used in M. Opher et al. (2009a).

The model used here also uses a four-fluid treatment of neutral hydrogen (similar to M. Opher et al. 2009b), but unlike the previous works, we model the plasma as two ion fluids, thermal ions and pickup ions, rather than a single-ion fluid. The separate pickup ion fluid allows the model to more accurately capture the fact that the pickup ions form a distinct, hot component of the solar wind plasma. The multi-ion model used here, originally implemented in M. Opher et al. (2020), was extended in E. Bair et al. (2024, in preparation) to include a separate electron pressure. Here, we assume that the electrons are “cold,” with their temperature equal to the proton temperature. The assumption of “cold” electrons is widely used in models of the heliosphere (M. Opher et al. 2020; F. Fraternali et al. 2023), but some works argue for “hot” electrons (H. J. Fahr et al. 2014; B. Zieger et al. 2015). For a

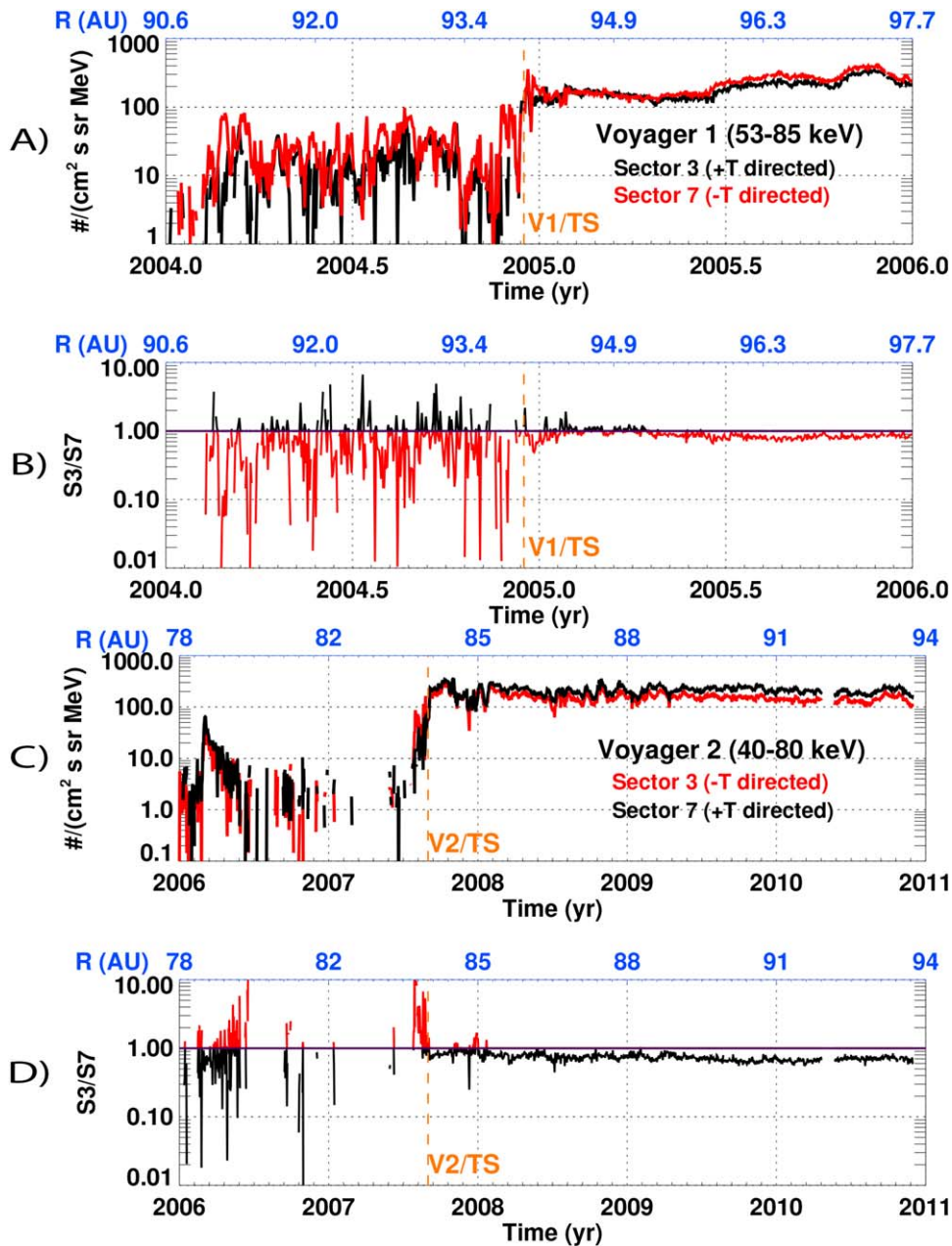


Figure 1. (A) V1 LECP observations as the spacecraft approached the TS. The red line is observations of sector 7 ($-T$ direction). The black line is observations of sector 3 ($+T$ direction). The orange dashed line is the TS location. (B) Plot over time of the ratio of sector 3 to sector 7. The line is red when sector 7 dominates over sector 3 observations, indicating primarily $-T$ beaming, and the line is black when sector 3 dominates over the sector 7 observations, indicating primarily $+T$ beaming. (C) The same as panel (A) but for V2 approaching the TS. (D) The same as panel (B) but for V2 approaching the TS.

detailed exploration of the effect of a separate electron equation and “hot” electrons, see E. Bair et al. (2024, in preparation).

The simulation coordinates are the Cartesian heliographic inertial frame. The x -axis is oriented along the line of intersection between the solar equatorial plane and the ecliptic equatorial plane, the z -axis is aligned with the solar rotation axis, and the y -axis is the right-hand-rule complement of x and z . The domain of the simulation is ± 2000 au in the y and z directions and ± 1500 au in the x direction. This domain extent is necessary to capture the slow bow shock/wave when it is present (B. Zieger et al. 2013). The solar wind conditions are implemented as spherically symmetric inner boundary conditions at 30 au, while ISM conditions are implemented as the outer boundary conditions at the face of the domain in the $-x$ direction.

We use Adaptive Mesh Refinement to capture regions of interest with higher resolution. The resolution is as small as 0.35 au at the inner boundary and increases in size, with the largest grid cell being 46.875 au at the outer boundary. The grid is refined at the TS crossings for each of the spacecraft trajectories. These refinements reduce the grid at the crossing to 0.35 au. This refinement is necessary to minimize the uncertainty in our positions due to grid size.

This model uses the same solar wind and pristine ISM conditions as M. Opher et al.’s (2020) “Case B.” For the solar wind conditions, we assume a spherically symmetric, fully ionized solar wind with a density of $8.74 \times 10^{-3} \text{ cm}^{-3}$, a velocity of 417 km s^{-1} , and a temperature of $2 \times 10^4 \text{ K}$ for both the ions and electrons at 30 au. We also assume a Parker

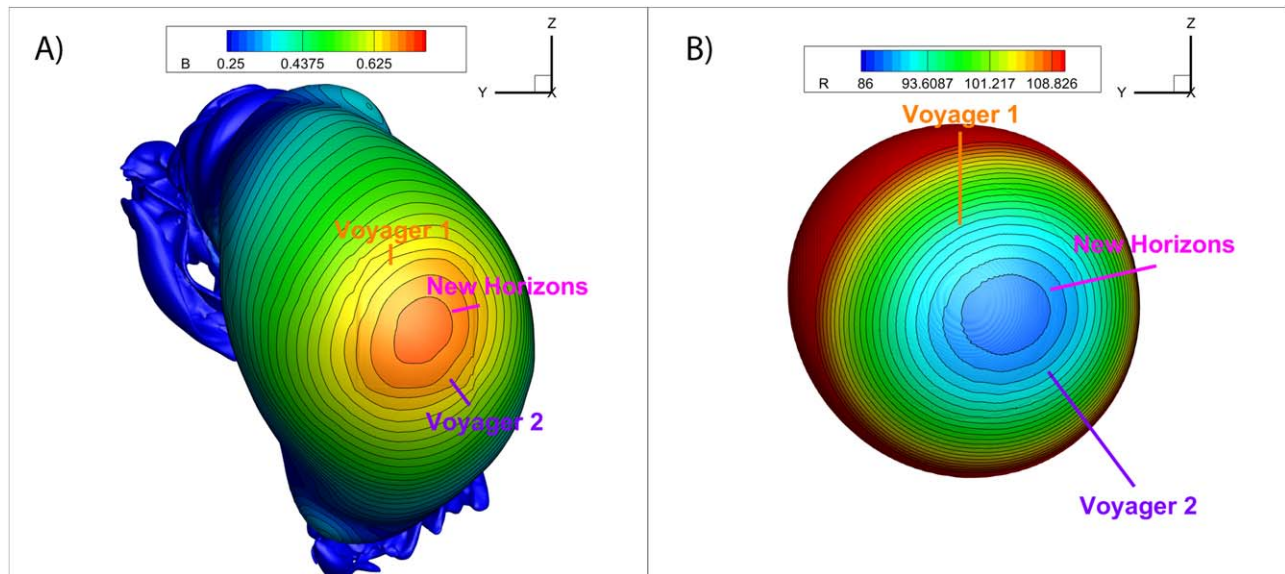


Figure 2. Trajectories for V1, V2, and NH as orange, purple, and magenta lines, respectively, cutting through surfaces representing the HP (A) and TS (B) showing the geometric differences between each trajectory. (A) Isosurface of temperature equal to 2.17×10^5 K representing the HP with contours of magnetic pressure with spacecraft trajectories projecting through the surface. (B) Isosurface of plasma speed equal to 350 km s^{-1} representing the TS with contours of radial distance.

spiral magnetic field configuration with a radial magnetic field strength of 7.17×10^{-3} nT, also at 30 au. For the pristine ISM the plasma density is 0.06 cm^{-3} , the neutral density is 0.18 cm^{-3} , the speed of both species is 26.4 km s^{-1} , and the temperature of both species is 6519 K. The ISM magnetic field lies in the hydrogen deflection plane (R. Lallement & J. L. Bertaux 2005; R. Lallement et al. 2010), with an angle between the magnetic field and ISM flow vector, α_{BV} , equal to 40° and an angle between the B - V plane and the solar equator plane, β , equal to 60° . We use an interstellar magnetic field strength of 0.32 nT. These values are used as they best reproduce the V1 and V2 observations in this work. The neutral and plasma components of the ISM flow together in the direction determined from undisturbed helium flowing through the heliosphere (R. Lallement & J. L. Bertaux 2005; R. Lallement et al. 2010).

For the analysis, we use the following procedure. First, we define the TS within our simulation. Since a numerical simulation does not have infinite resolution, the TS transition is spread across several discrete grid cells. To address the discretization of our simulation, we define the TS to be where the plasma speed, U , is equal to 350 km s^{-1} . This speed corresponds to the half distance across the shock. An isosurface of this speed, representing the TS, captures the fundamental asymmetric, nonspherical nature of the TS.

Then we determine two positions, p_{TS} and p_0 , along the trajectories of V1, V2, and NH. p_{TS} is the position along the trajectory where $U = 225 \text{ km s}^{-1}$, defining where the spacecraft crosses the TS. p_0 is the earliest position in time along the trajectory where a magnetic field line from the spacecraft location is connected upwind to the TS. This position is where the spacecraft would begin to observe TSPs.

3. Results

Our model results show significant asymmetric bluntness. The left panel of Figure 2 displays the HP with magnetic field strength contours, while the right panel shows the TS with radial distance contours. The minimum radial distance of the

TS is 87.1 au near the nose and increases to over 110 au in the flanks and tail. NH crosses the TS at 87.8 au, V1 at 93.1 au, and V2 at 90.4 au. The contours on the HP show a buildup of magnetic field strength that is slightly offset from the center. The magnetic field strength contours align well with the radial distance contours on the TS. The increased magnetic field strength, and therefore magnetic pressure, creates a higher total pressure that is transmitted through the heliosheath. As a result, the steady-state radial distance of the TS at this location is closer to the Sun to compensate for the increased pressure.

The specific geometry of the spacecraft trajectories through the TS plays a major role in determining how far ahead of the crossing the spacecraft will be connected to the TS and begin to observe TSP beaming. The trajectories of V1, V2, and NH are shown in Figure 2. V1 and V2 left the solar system at higher helioaltitudes than NH. Additionally, NH is predicted to cross the TS at a closer radial distance to the Sun than either V1 or V2 (neglecting time-dependent effects). In fact, the NH trajectory nearly passes through the closest point of the TS to the Sun.

When comparing our modeled TSP onset to observations, we will use 2.5 yr prior to crossing for V2 and 1.0 yr prior to crossing for V1. For V2, the observations of TSPs are consistent, making the timing easy to determine. However, for V1, the first observed TSPs were approximately 2.5 yr prior to crossing the TS, after which the TSP intensity significantly decreased for most of 2003. The 1.0 yr period corresponds to the time from which TSP reappeared and consistently increased until the crossing.

3.1. Steady-state Connectivity

Panel (A) of Figure 3 shows a plane parallel to the solar equatorial plane, positioned at the Z coordinate of the V1 crossing. The V1 trajectory (orange curve) and the TS (black solid curve) are plotted in this plane. Additionally, solar magnetic field lines are overlaid on the trajectory at various points prior to crossing. Since the shock is nonspherical, the magnetic field line connected to V1 at the TS crossing (red

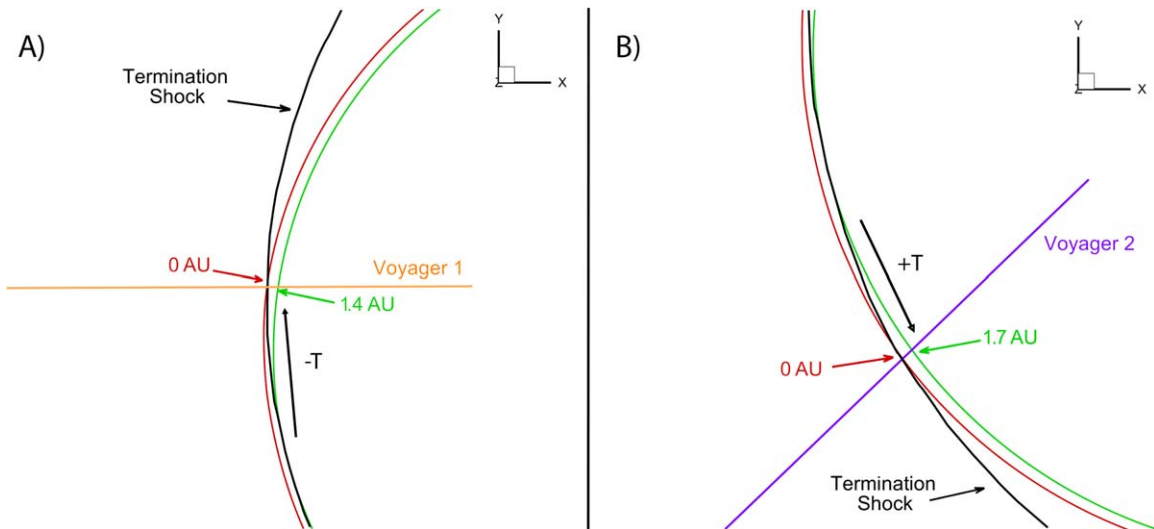


Figure 3. (A) Solar equatorial plane (Z plane) at the TS crossing of V1. The black solid line represents the nonspherical TS in this plane. The orange line represents the trajectory of V1. The red and green lines represent solar magnetic field lines along the V1 trajectory at 0 and 1.4 au from crossing the TS, respectively. (B) Same as panel (A) but at the TS crossing of V2. The purple line represents the V2 trajectory, and the red and green lines represent solar magnetic field lines connected to Voyager 20 and 1.7 au from the crossing the TS, respectively.

curve, labeled 0 au) is downstream of the TS on one side of the trajectory and upstream of the TS on the other. The magnetic field line that connects V1 to the TS the earliest along the trajectory (green curve, labeled 1.4 au) indicates the earliest point along the V1 trajectory that the spacecraft would begin to observe streaming TSPs upwind of the TS. This corresponds to 0.4 yr prior to crossing the TS for V1, which is less of a warning than observed. Our model predicts that from this point onward, V1 would have observed accelerated particles streaming in the $-T$ direction, consistent with the observations.

Since these simulations are not infinitely resolved, and the simulation is run using a second-order scheme, the distances should have an associated uncertainty of twice the grid size. The grid at the crossings is 0.35 au, which corresponds to an uncertainty of 0.7 au. This uncertainty is relatively small compared to the larger uncertainty in accounting for a moving TS.

Similarly, for V2, the nonspherical shock causes magnetic field lines to connect the spacecraft to the TS prior to the crossing. Panel (B) of Figure 3 is the same as panel (A), except that the spacecraft trajectory plotted is for V2 rather than V1 and the plane is at the Z coordinate of the V2 TS crossing. For the V2 trajectory, due to different latitude and longitude of the spacecraft trajectory compared to V1, the earliest field line connected to the TS (green curve) is 1.7 au from the shock rather than 1.4 au. This corresponds to 0.54 yr prior to crossing the TS, which is less of a warning than observed. Due to the direction the magnetic field connects to the TS, our model predicts that V2 would observe particles beaming from the $+T$ direction. This direction is supported by observations.

Figure 4 presents our prediction for the NH crossing (magenta). The NH trajectory has a similar heliolongitude to V2 but at a smaller heliolatitude. The magnetic field connects NH to the TS in the same direction as V2, indicating that NH will also see TSPs streaming in the $+T$ direction. Our steady-state model predicts a 1.0 au warning prior to crossing the TS, corresponding to a 0.34 yr warning. NH has to be closer the TS to observe TSPs than either V1 or V2.

Although our steady-state model predicts the correct direction for the streaming of TSPs for V1 and V2 ($-T$ and $+T$, respectively), the predicted timings of the observations, 0.54 and 0.38 yr for V1 and V2, respectively, do not align with the observations, ~ 2.5 and ~ 1 yr for V1 and V2, respectively. Table 1 summarizes these findings and compares them to the previous work of M. Opher et al. (2006). This implies that while the ISM magnetic field accounts for some of the east-west asymmetry in the observations, time-dependent modeling is required to close the gap between models and observations. In the next section, we will constrain the speed of TS during these crossings and the implication for the NH TS crossing.

3.2. Constraining the TS Speed at the V2 TS Crossing

A moving TS is needed to close the gap between the modeled distance to the TS and where TSPs were observed. This is consistent with our understanding of the TS as a dynamic surface that responds to the changing solar wind conditions propagated from the Sun. However, modeling the highly variable solar wind is a difficult task, and various approaches have been used. Works such as J. D. Richardson & C. Wang (2011), H. Washimi et al. (2011), V. V. Izmodenov & D. B. Alexashov (2020), and E. Provornikova et al. (2014) all implement time-dependent solar wind using different methods and each get different solutions. These models agree on the broad motion of the TS over a solar cycle, but the motion of the TS on timescales of less than 1 yr can differ.

This makes applying time-dependent modeling to TSP observations difficult as different models yield different solutions. However, we can constrain the time-dependent motion of the TS using the TSP observations made by V2 just prior to the TS crossing. We use the V2 observations because the intensity of the TSPs steadily increased from the onset of the observations until the TS crossing. This suggests that V2 was magnetically connected to the TS the entire duration of these observations.

Figure 5 shows a cartoon diagram showing the configuration of V2 and the TS when TSPs begin to be observed and when V2 crosses the TS. V2 began observing TSPs at approximately

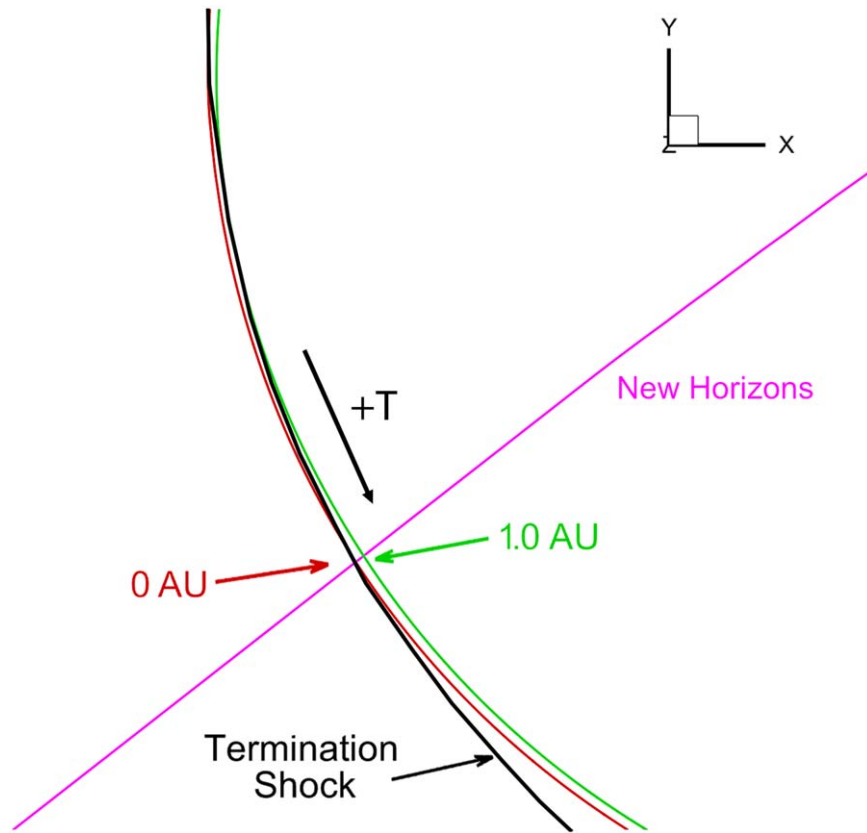


Figure 4. Similar to Figure 3 but at the NH TS crossing. The magenta line represents the NH trajectory. The red and green lines represent the solar magnetic field lines connected to NH 0 and 1.0 au from crossing the TS, respectively.

Table 1.
Beaming Direction and Distance

	V1 Distance, Direction	V2 Distance, Direction	NH Distance, Direction
Observations	3–4 au, $-T$	5–6 au, $+T$	N/A
Model excl. Neutrals	3 au, $-T$	5 au, $+T$	N/A
Model incl. Neutrals	1.4 ± 0.7 au, $-T$	1.7 ± 0.7 au, $+T$	1.0 ± 0.7 au, $+T$

Note. Predicted and observed upstream distance from the TS and beaming direction where TSPs are observed at V1, V2, and NH. Each of the predicted distances have an associated uncertainty of 0.7 au due to grid resolution.

75.4 au from the Sun. From our steady-state modeling, we know that V2 had to be less than 1.7 au from the TS for these observations to begin. We also know the location of V2 at the TS crossing crossing was 83.7 au. This means the TS had to travel radially outward 6.6 au in 2.66 yr at a speed of 2.5 au yr^{-1} .

This means that V2 was able to observe TSPs for a longer period than suggested solely due to the east–west asymmetry, due to the TS moving outward during the crossing. H. Washimi et al. (2011) and J. D. Richardson & C. Wang (2011) both show similar outward motion of the TS at times very near the crossing in their models. Interestingly, on larger timescales, the TS is actually moving inward.

In the best-case scenario for the NH TS crossing, the TS would be moving radially outward as the spacecraft approaches it, prolonging TSP observations and providing a longer

warning of the upcoming TS crossing. In the worst-case scenario, the TS would be moving radially inward as NH approaches it, reducing the effective warning time from TSPs. Using the V2 TS speed of 2.48 au yr^{-1} and the distance from the TS for NH to observe TSPs (1.0 au), we can calculate the warning time for each scenario. The best-case scenario would provide a warning of 2.4 yr, slightly less than what V2 observed. The worst-case scenario would result in a warning of only 0.2 yr, or about 2 months.

4. Discussion

In this work, we presented a similar analysis to that of M. Opher et al. (2006) and M. Opher et al. (2007) but with a significantly updated model. It was suggested that including neutral hydrogen into these models would reduce the bluntness of the TS and, as a result, decrease the distance at which V1 and V2 would be connected to the TS upwind (N. V. Pogorelov et al. 2007, 2008a, 2008b). Our model with neutrals shows that V1 and V2 needed to be closer to the TS to be magnetically connected. Although it is true that the inclusion of neutrals does symmetrize the TS, some of the asymmetry, due to the interstellar magnetic field, remains.

We calculate the speed of the TS using the V2 observations because the observations clearly show that TSPs were consistently observed from the onset of TSPs until the TS crossing. This consistency allows us to assume the spacecraft remained magnetically connected to the TS throughout the observations. However, we are unable to apply this assumption to the V1 observations. In the V1 observations, there is a significant decrease in the intensity of TSPs in 2003. This could

TSP observation just prior to V2 TS crossing

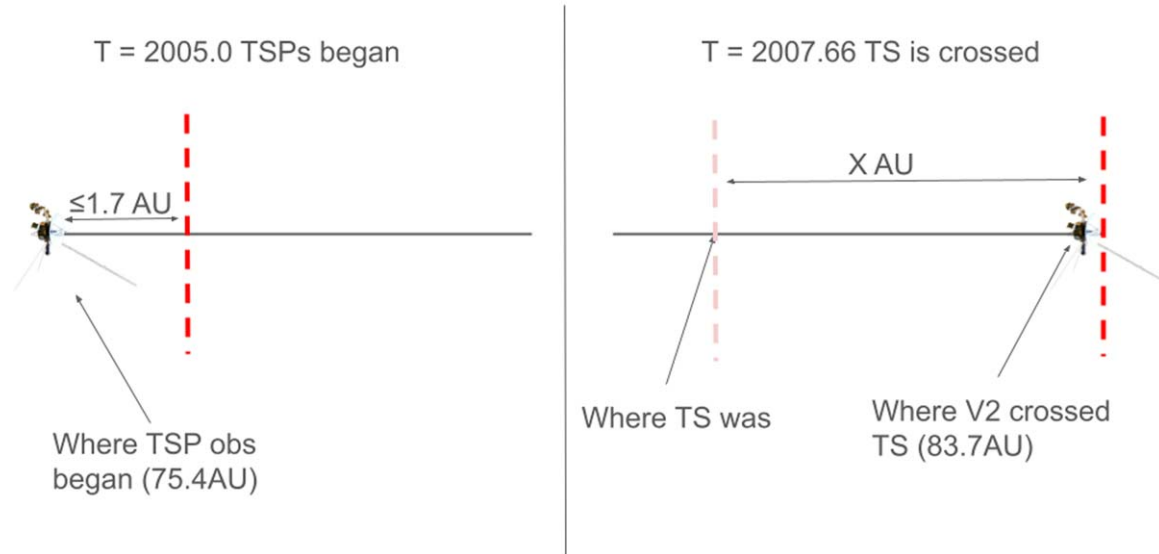


Figure 5. Cartoon depicting the TSP observations for V2. Left: configuration of V2 and the TS when V2 first observes TSPs. Right: configuration of V2 and the TS when V2 crosses the TS showing how far the TS must have moved.

suggest that V1 was only briefly connected to the TS in 2002, then TS then moved radially outward at a speed faster than the V1 spacecraft, magnetically disconnecting the spacecraft. Later, V1 caught up to the TS, allowing observations to resume until the TS crossing. This interpretation depends on whether the TSP observations fully ceased, highlighting the need for future work to reexamine these observations.

It is important to recognize that alternative explanations for the observed phenomena have also been proposed. One notable suggestion is that the time-dependent solar wind can cause the TS to be turbulent. In this scenario, a turbulent TS could periodically connect to the spacecraft prior to the spacecraft being close enough to connect with a stable TS. However, this explanation does not negate the geometric effect studied here; rather, it could enhance it. What we present here is a geometrically driven minimum distance at which the spacecraft would connect to the TS. A turbulent TS could allow a spacecraft to connect to the TS even earlier than predicted here.

5. Conclusion

In this Letter, we use the solution of a multi-ion MHD heliosphere model to investigate TS crossings. Due to the interstellar magnetic field, the nose of the TS is pushed in, causing the TS to be asymmetric and blunt. This asymmetry, in combination with the specific trajectories of V1, V2, and NH, makes each of their TS crossings distinct. Although our model shows reduced east–west asymmetry, due to the inclusion of neutral hydrogen, the east–west asymmetry still contributes to the differences in observations for V1 and V2.

Our model predicts that V1 would observe TSPs beaming in the $-T$ direction 1.4 au prior to crossing the TS due to just the geometry of the TS and the trajectory. This prediction is closer than prior works that did not include neutral hydrogen (M. Opher et al. 2006; 3 au, $-T$ direction) and observations (3–4 au, $-T$ direction) but in the correct direction. For V2, our model predicts the spacecraft would have observed TSPs beaming in the $+T$ direction 1.7 au prior to crossing the TS. This is closer to the TS than prior works that did not include

neutral hydrogen (M. Opher et al. 2006; 5 au, $+T$ direction) and observations (5–6 au, $+T$ direction) but in the correct direction. This implies that static solar wind is not able to reproduce these observations alone. For the NH TS crossing, our model predicts that TSPs will be observed streaming in the $+T$ direction 1.0 au prior to crossing the TS. This is the same direction as the V2 observations but at a closer distance to the TS. These results are summarized in Table 1.

Using the V2 observations, we were able to determine the TS must have been moving at ~ 2.5 au yr $^{-1}$ outward during the TSP observations. Using this speed we were able to determine the worst-case scenario and best-case scenario for the NH TS crossing. The worst-case scenario, the TS moving inward at this speed during the crossing, only had a 0.2 yr warning prior from TSP observations. The best-case scenario, the TS moving outward during the crossing, had a 2.4 yr warning, slightly shorter than the V2 observations.

Acknowledgments


This project was supported by the NASA grant 18-DRIVE-2-0029 as part of the NASA DRIVE Center titled “Our Heliospheric Shield.” Also, support was provided through the FINESST award 19-HELIO20-0023. For more information about this center, please visit <https://shielddrivecenter.com/>. We also thank NASA for support of several coauthors of this Letter via the New Horizons project. K.D. was supported through JHU/APL by NASA under contracts NAS5 97271, NNX07AJ69G, and NNN06AA01C and by a subcontract at the Center for Space Research and Technology.

ORCID iDs

Erick Powell <https://orcid.org/0009-0008-8209-5117>
 Merav Opher <https://orcid.org/0000-0002-8767-8273>
 Ethan Bair <https://orcid.org/0000-0003-0610-1382>
 Matthew Hill <https://orcid.org/0000-0002-5674-4936>
 Romina Nikoukar <https://orcid.org/0000-0002-8608-2822>
 Joe Giacalone <https://orcid.org/0000-0002-0850-4233>

Konstantinos Dialynas  <https://orcid.org/0000-0002-5231-7929>

John D. Richardson  <https://orcid.org/0000-0003-4041-7540>

Pontus C. Brandt  <https://orcid.org/0000-0002-4644-0306>

Kelsi N. Singer  <https://orcid.org/0000-0003-3045-8445>

S. Alan Stern  <https://orcid.org/0000-0001-5018-7537>

Elena Provornikova  <https://orcid.org/0000-0001-8875-7478>

Anne J. Verbiscer  <https://orcid.org/0000-0002-3323-9304>

Andrew R. Poppe  <https://orcid.org/0000-0001-8137-8176>

Joel Wm. Parker  <https://orcid.org/0000-0002-3672-0603>

References

- Axford, W. I. 1972, *The Interaction of the Solar Wind With the Interstellar Medium*, Vol. 308 (Washington, DC: NASA), 609
- Baranov, V. B., & Malama, Y. G. 1993, *JGR*, **98**, 15157
- Burlaga, L. F., Ness, N. F., Acuña, M. H., et al. 2005, *Sci*, **309**, 2027
- Burlaga, L. F., Ness, N. F., Acuña, M. H., et al. 2008, *Natur*, **454**, 75
- Davis, L. 1955, *PhRv*, **100**, 1440
- Decker, R. B., Krimigis, S. M., Roelof, E. C., et al. 2005, *Sci*, **309**, 2020
- Decker, R. B., Krimigis, S. M., Roelof, E. C., et al. 2008, *Natur*, **454**, 67
- Dialynas, K., Krimigis, S. M., Decker, R. B., et al. 2022, *SSRv*, **218**, 21
- Dialynas, K., Krimigis, S. M., Mitchell, D. G., Decker, R. B., & Roelof, E. C. 2017, *NatAs*, **1**, 0115
- Drake, J. F., Swisdak, M., & Opher, M. 2015, *ApJL*, **808**, L44
- Fahr, H. J., Chashei, I. V., & Verscharen, D. 2014, *A&A*, **571**, A78
- Fraternali, F., Pogorelov, N. V., & Bera, R. K. 2023, *ApJ*, **946**, 97
- Galli, A., Baliukin, I. I., Bzowski, M., et al. 2022, *SSRv*, **218**, 31
- Izmodenov, V. V., & Alexashov, D. B. 2015, *ApJS*, **220**, 32
- Izmodenov, V. V., & Alexashov, D. B. 2020, *A&A*, **633**, L12
- Izmodenov, V. V., Malama, Y. G., Kalinin, A. P., et al. 2000, *Ap&SS*, **274**, 71
- Jokipii, J. R., Giacalone, J., & Kóta, J. 2004, *ApJL*, **611**, L141
- Krimigis, S. M., Decker, R. B., Roelof, E. C., et al. 2019, *NatAs*, **3**, 997
- Lallement, R., Quémerais, E., Bertaux, J. L., et al. 2005, *Sci*, **307**, 1447
- Lallement, R., Quémerais, E., Koutroumpa, D., et al. 2010, in *AIP Conf. Ser.* 1216, *Twelfth Int. Solar Wind Conf.*, ed. M. Maksimovic et al. (Melville, NY: AIP), 555
- Opher, M., Bibi, F. A., Toth, G., et al. 2009a, *Natur*, **462**, 1036
- Opher, M., Drake, J. F., Zieger, B., & Gombosi, T. I. 2015, *ApJL*, **800**, L28
- Opher, M., Liewer, P. C., Gombosi, T. I., et al. 2003, *ApJL*, **591**, L61
- Opher, M., Loeb, A., Drake, J., & Toth, G. 2020, *NatAs*, **4**, 675
- Opher, M., Richardson, J. D., Toth, G., & Gombosi, T. I. 2009b, *SSRv*, **143**, 43
- Opher, M., Stone, E. C., & Gombosi, T. I. 2007, *Sci*, **316**, 875
- Opher, M., Stone, E. C., & Liewer, P. C. 2006, *ApJL*, **640**, L71
- Parker, E. N. 1961, *ApJ*, **134**, 20
- Pogorelov, N. V., Borovikov, S. N., Heerikhuisen, J., & Zhang, M. 2015, *ApJL*, **812**, L6
- Pogorelov, N. V., Heerikhuisen, J., & Zank, G. P. 2008a, *ApJL*, **675**, L41
- Pogorelov, N. V., Stone, E. C., Florinski, V., & Zank, G. P. 2007, *ApJ*, **668**, 611
- Pogorelov, N. V., Zank, G. P., & Ogino, T. 2008b, *AdSpR*, **41**, 306
- Provornikova, E., Opher, M., Izmodenov, V. V., Richardson, J. D., & Toth, G. 2014, *ApJ*, **794**, 29
- Richardson, J. D., Kasper, J. C., Wang, C., Belcher, J. W., & Lazarus, A. J. 2008, *Natur*, **454**, 63
- Richardson, J. D., & Wang, C. 2011, *ApJL*, **734**, L21
- Stone, E. C., Cummings, A. C., McDonald, F. B., et al. 2005, *Sci*, **309**, 2017
- Stone, E. C., Cummings, A. C., McDonald, F. B., et al. 2008, *Natur*, **454**, 71
- Swaczyna, P., McComas, D. J., Zirnstein, E. J., et al. 2020, *ApJ*, **903**, 48
- Tóth, G., Sokolov, I. V., Gombosi, T. I., et al. 2005, *JGRA*, **110**, A12226
- Tóth, G., van der Holst, B., Sokolov, I. V., et al. 2012, *JCoPh*, **231**, 870
- Washimi, H., Zank, G. P., Hu, Q., Tanaka, T., & Munakata, K. 2007, *ApJL*, **670**, L139
- Washimi, H., Zank, G. P., Hu, Q., et al. 2011, *MNRAS*, **416**, 1475
- Witte, M. 2004, *A&A*, **426**, 835
- Zank, G. P., Heerikhuisen, J., Wood, B. E., et al. 2013, *ApJ*, **763**, 20
- Zieger, B., Opher, M., Schwadron, N. A., McComas, D. J., & Tóth, G. 2013, *GeoRL*, **40**, 2923
- Zieger, B., Opher, M., Tóth, G., Decker, R. B., & Richardson, J. D. 2015, *JGRA*, **120**, 7130